

Behavior of a One-Sixth Scale Wood-Framed Residential Structure under Wave Loading

Jebediah S. Wilson¹; Rakesh Gupta, M.ASCE²; John W. van de Lindt, M.ASCE³; Milo Clauson⁴; and Rachel Garcia⁵

Abstract: The goal of this study was to develop an understanding of the nature of wave loading on a wood-framed scale residential building model for a variety of building configurations and test conditions. Testing was performed on a 1/6th scale two-story wood-framed residential structure. The structure was impacted with waves and tested in both flooded and nonflooded conditions. The measured forces were mainly uplift forces due to wave loading, and resulting overturning moments. The qualitative analysis of the data showed that differences in structural stiffness throughout the structure will cause a different load distribution in the structure, e.g., overhanging eaves above the garage can provide unanticipated loading conditions, water traveling beneath the structure generates predominantly uplift forces, and the effect of waves breaking on or near the structure greatly increases the loading. The ratio of force from the windows closed condition to the windows open condition is approximately 2.5:1.

DOI: 10.1061/(ASCE)CF.1943-5509.0000039

CE Database subject headings: Buildings, residential; Wood structures; Frames; Floods; Structural behavior.

Introduction

On August 23, 2005, Hurricane Katrina moved inland with wind speeds as high as 225 km/h (National Weather Service 2005). The effects of its devastation were seen as far as 160 km inland with the worst damage seen in New Orleans, La. An in-depth examination of the effects of wind loading on structures in the Gulf Coast region in the aftermath of Hurricane Katrina was led by van de Lindt et al. (2007). They determined that although wind was a significant destructive force, the damage from waves posed a much higher threat to wood-framed structures not designed for wave loading. In most cases near the coast, they observed that waves completely removed structures from their foundations, and reduced homes into piles of disconnected lumber.

As higher percentages of the United States population move into coastal regions, the need to build infrastructure to withstand wave loading becomes increasingly important. Engineers design buildings to resist a variety of loading conditions. The methods for determining these loads are detailed in ASCE/SEI 7-05 (ASCE 2005). This publication has 60 pages detailing wind load-

ing and more than 100 pages on seismic loading (over 12 chapters). The same document has only five pages on flood loading, with two pages specifically on wave loading. The wave guidelines detailed in ASCE/SEI 7-05 only discuss breaking waves (waves in transition from nonbroken, potential flow, to broken, quasi-steady turbulent bore) with no details on loading calculations for broken waves (waves with quasi-steady turbulent bore) or how to apply the loading to wood-framed structures. The City and County of Honolulu Building Code (HBC 2000) has developed more detailed design guidelines for wave loading, yet evidence indicates this overpredicts forces (Yeh et al. 2005). There is ample need for further research to understand and detail the forces generated from wave loading. Although homeowners may not be required to build structures to withstand the force of many natural disasters, increased research may enable further protection of lives from these events.

The study summarized herein sought to further understand wave loading on wood-framed structures. Specifically, the objectives of this project were (1) to measure forces exerted on a 1/6th scale, two-story, wood-framed residential structure when subjected to a waves; (2) to evaluate qualitatively the structural response to different loading conditions; and (3) to compare the effects of different structural configurations on the structural response. It should be noted that this study only relates force data to the model structure, not the full-size structure, i.e., describing the qualitative behavior of a small-scale structure under wave loading.

In the past wave loading was studied as it pertained to off shore structures. Little research has been done involving broken waves impacting upon structures. This is mainly because structures are built far enough from shore to avoid these conditions, yet tsunamis and hurricanes bring these waves inland. It is also difficult to study this type of loading as the facilities are few and expensive. The Coastal Construction Manual (CCM) (FEMA 2005) provides some provision for calculating design loads including flood loads. The CCM does not deal with loading from solitary bores (turbulent feature on the face of a broken wave) in

¹Former Graduate Research Assistant, Dept. of Wood Science and Engineering, Oregon State Univ., Corvallis, OR 97331.

²Professor, Dept. of Wood Science and Engineering, Oregon State Univ., Corvallis, OR 97331 (corresponding author). E-mail: rakesh.gupta@oregonstate.edu

³Associate Professor, Dept. of Civil Engineering, Colorado State Univ., Fort Collins, CO 80523.

⁴Senior Faculty Research Assistant, Dept. of Wood Science and Engineering, Oregon State Univ., Corvallis, OR 97331.

⁵Former Graduate Research Assistant, Dept. of Civil Engineering, Colorado State Univ., Fort Collins, CO 80523.

Note. This manuscript was submitted on December 3, 2008; approved on March 21, 2009; published online on March 28, 2009. Discussion period open until March 1, 2010; separate discussions must be submitted for individual papers. This paper is part of the *Journal of Performance of Constructed Facilities*, Vol. 23, No. 5, October 1, 2009. ©ASCE, ISSN 0887-3828/2009/5-336-345/\$25.00.

a nonflooded condition, and thus is of little use in estimating wave forces for this study. ASCE 7–05 also deals with flood loading but includes details on breaking wave loads which is more suited to offshore structures.

Wydajewski (1998) tested prototype scale breakaway walls of wood construction. He worked with nonbreaking waves, breaking waves and broken waves. He developed theoretical force predictions and made comparisons to measured forces and moments. He warns of difficulty knowing if a wave is fully broken or still breaking, leading to large differences in measured forces.

Ramsden (1993) measured forces on a vertical wall due to long waves, bores, and dry-bed surges. Like Wydajewski, Ramsden directly measured the lateral force instead of calculating the force from pressure measurements. Ramsden has the advantage of getting accurate wave height measurements using a laser-induced fluorescence system, yet despite this technology there is still related difficulty in determining the maximum wave runup (maximum vertical extent of wave uprush on a beach or structure above the still water level) height on the vertical wall. Ramsden used theoretical equations from Goring (1979) for determining the force and moment, which were compared to measured values. One of the major conclusions from this work indicates that the force computed assuming purely hydrostatic conditions and using the maximum wave runup height exceeded the maximum measured values in all cases. This was thought to be due to part of the force being vertical during wave runup. Ramsden found that the theoretical equations developed by Su and Mirie (1980), were the closest fit to the measured values of force and moment.

Arnason (2005) studied interactions between an incident bore and a free-standing coastal structure. That work also focuses on qualitative observations regarding the structures response to wave loading. In the controlled environment of a small wave flume (hydraulic wave flume with long aspect ratio), theoretical predictions of wave height and force aligned well with theory. Yet having a narrow channel means the water didn't travel naturally around the structure as would happen if the structure were isolated. Future studies might test several structures side by side, as might be found in a housing community to see how loading was affected.

Most closely related to this study is the recent work of Thusy-anthan and Madabhushi (2008). This research utilizes a small tsunami wave tank measuring 4.5 m long with waves generated by dropping a 100-kg block in the water. Model coastal structures scaled at 1:25 were tested. One structure was designed similar to a common Sri Lankan house and one structure attempted to model a new tsunami resistant structure. Water was allowed to pass through and under the tsunami resistant model, effectively reducing the loading. Pressure sensors were used at two locations on the face of the model and at one location on the back. Results indicate that the tsunami resistant model was successful at reducing forces and survived the wave impact, while the typical Sri Lankan model was destroyed or displaced from its foundation. This indicates a need to examine how building configuration could be used to better withstand wave loading.

Materials and Methods

This study used a structurally compliant 1/6th scale model of a two-story residential structure. The structure was constructed using light-framed wood construction similar to that found in coastal regions in the United States. Garcia (2008) performed the scaling procedures which allowed approximate structural compli-



Fig. 1. Construction sequence (a) assemble first floor walls; (b) assemble second floor; (c) lower second floor on top of first floor; and (d) completed structure

ance similar to a full-scale residential building. Complete details can be found in Wilson (2008).

Model Structure Construction

The wall framing members were constructed of 0.95 cm \times 1.9 cm pine boards, and the roof framing members were constructed of 1.3 cm \times 1.9 cm pine boards. The scaled wall sheathing was made from oriented strand board cut to 0.5 cm thick \times 20 cm wide \times 43 cm high, effectively modeling a 120 cm \times 240 cm wall panel typical of exterior sheathing. Roof and floor diaphragm sheathing was made from 0.64 cm plywood. The framing connections were made with 1 mm \times 25.4 mm staples, with wall sheathing attached using 1 mm \times 13 mm steel brad nails. The walls were assembled on a 1.3 cm \times 110 cm \times 240 cm steel plate. The plate was used as slab on ground foundation or crawl space type foundation depending upon whether metal flashing was used around it or not. Walls were attached to the steel plate using 3 mm \times 25 mm stainless steel anchor bolts through the bottom plate of the walls at every 125 mm based on the prescribed spacing for 209 km/h (130 mph) prescriptive code [American Forest and Paper Association (AFPA) 2006]. The second floor diaphragm was then attached using thin gauge sheet metal plates every 30 cm. The second floor walls were stapled to the second floor diaphragm using 1 mm \times 25 mm staples, again using spacing (every 125 mm) from 209 km/h prescriptive code. The roof diaphragm was then attached using thin gauge sheet metal joist hangers. The construction sequence is shown in Fig. 1. The final dimensions of the structure are 240 cm long \times 110 cm wide \times 120 cm high (aspect ratio \sim 2:1). The model has several structural irregularities, including a reentrant corner near the front door and a second story floor diaphragm that doesn't extend over the garage.

Testing

Testing was performed at the Oregon State University tsunami wave basin (TWB), and involved impacting the wood structure with a series of waves and recording the force in four load cells

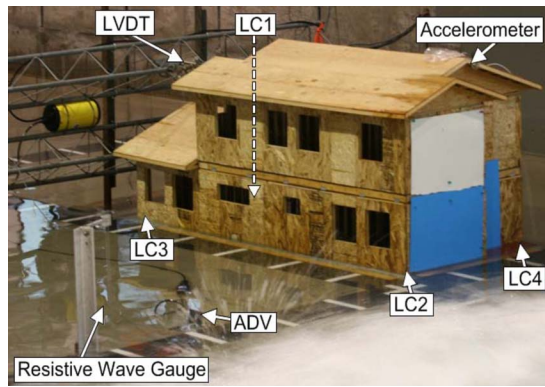


Fig. 2. Instrumentation for testing at Tsunami Wave Basin

(LC1, LC2, LC3, LC4), deflection (Δ_{wave}), acceleration, bore height, and wave velocity. See Fig. 2 for the wave lab testing instrumentation details.

Wave Lab Test Setup

The TWB layout, showing plan and elevation views of the testing area, is shown in Fig. 3. In this study, the wave maker generated 10-, 20-, 30-, 40-, 50-, and 60-cm solitary waves (a shallow water wave that consists of a single displacement of water) in both a 1-m and 1.1-m water depth. The structure was placed on a flat testing area with its front edge 10 cm back from the water's edge. This was done so the waves would have broken by the time they reach the structure, yet would still have much of their initial energy.

In this study, the goal was to examine many different testing configurations to determine the most suitable for data collection. The structure was tested with its long face toward the oncoming waves, hereafter referred to as the 0° orientation, as well as ro-

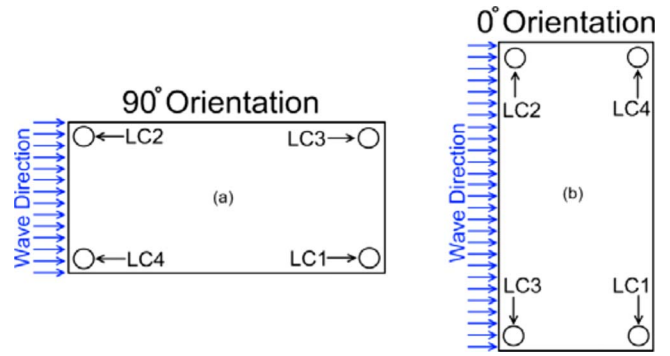


Fig. 4. Orientation and load cell locations with respect to wave direction (a) 90°; (b) 0°

tated 90° to put the short face to the oncoming waves, hereafter referred to as the 90° orientation, as shown in Fig. 4.

The structure had openings at window and door locations, which were covered in some trials by rigid plastic to simulate boarded windows. There was approximately a 4-cm gap beneath the steel plate necessitated by the placement of the load cells, which in some trials was covered by a thin gauge sheet metal flashing to prevent water intrusion beneath the plate. This modeled the presence of an open crawlspace versus a slab/stem wall foundation. In several trials the structure was raised an additional 5 cm using rigid aluminum risers to simulate the effects of a slightly elevated structure.

Throughout the following sections, the abbreviations listed below are used to indicate the specific testing configuration: 90 = 90° Orientation; 0 = 0° Orientation; 1.0 = 1.0 m water depth; 1.1 = 1.1 m water depth; WO = Windows open; WC = Windows closed; F = Flashed; NF = Not Flashed; E = Elevated structure (base plate ~10 cm above concrete floor); NE = Nonelevated Structure

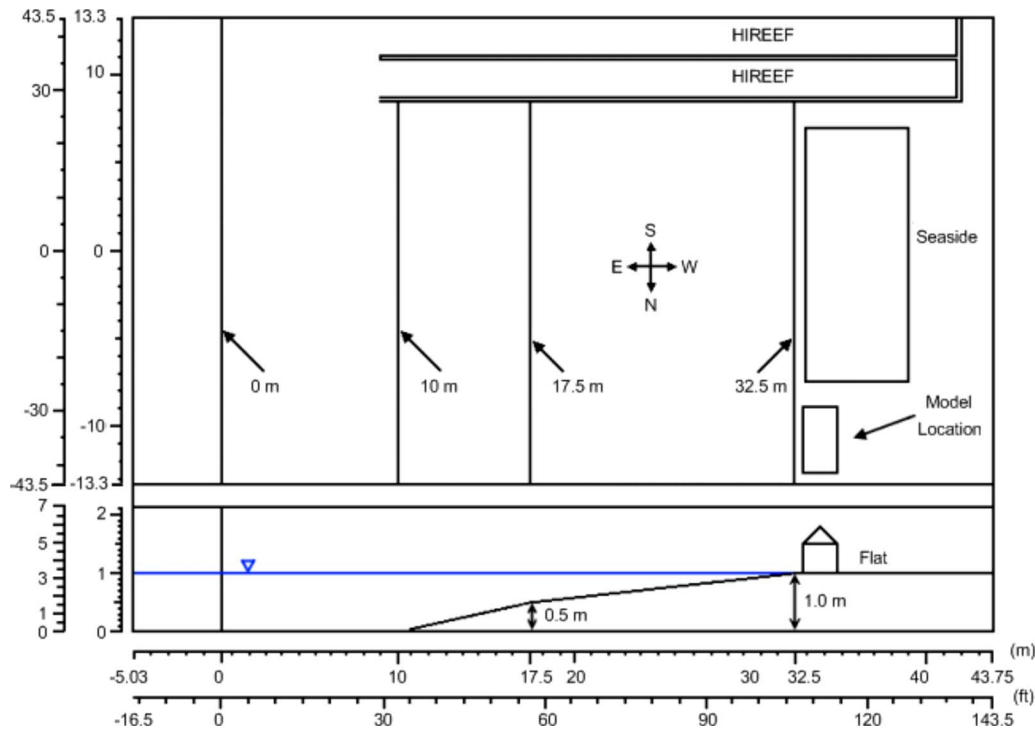


Fig. 3. Elevation and profile view of testing area at Tsunami Wave Basin

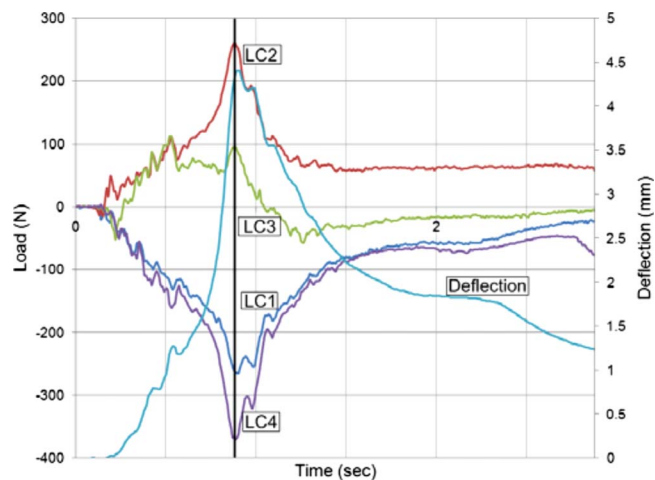


Fig. 5. Example plot generated from 40-cm wave with 0-1.0-WC-F-NE configuration

(base plate 4 cm above concrete floor). Example: 90-1.1-WC-F-NE indicates a test conducted in the 90° orientation, with the water level at 1.1 m, window and door coverings installed, base plate flashed to prevent water intrusion, and the structure fixed to the foundation in a nonelevated position. The flooded condition is indicated by 1.1 m water depth (1.1) and a nonelevated structure (NE).

Test Details

Force was measured using four uniaxial load cells (LC1–LC4) placed in each corner beneath the structure, effectively measuring the tension and compression forces generated by the waves impacting the structure. Deflection (Δ_{wave}) was measured at the second story roofline using a linear variable differential transformer (LVDT). Acceleration was measured on the second story roof near the front face of the structure using an accelerometer. Wave height was measured using a resistive wave gauge (surface pierc-

ing gauge used to measure wave height), and wave velocity was measured using an acoustic Doppler velocimeter. Fig. 2 shows the experimental setup. Raw voltages were sent from the instrumentation through an amplifier into a National Instruments data acquisition card. The amplified voltages were then sent through a PC and recorded as text files using LabView version 8.0. Testing at the TWB took place over 9 days. A total of 142 trials were conducted. There were 43 trials in the 0° orientation and 99 trials in the 90° orientation.

Results and Discussion

Fig. 5 shows an example of the data captured from a 40-cm-high wave with a 0-1.0-WC-F-NE configuration. The black, vertical line indicates the time of maximum loading. Values for all of the instruments at the time of maximum loading were collected, averaged, and exported from the individual files to a compiled summary sheet, as seen in Tables 1 and 2 (positive is tension and negative is compression). Due to large number of trials and scheduling issues, data for several wave heights were not collected. Those entries remain empty in Tables 1 and 2. It should be mentioned that this omission does not affect the trends and therefore the conclusions based on those trends. Plots from all the wave lab trials and other details about the project can be found in Wilson (2008).

During testing done in the 0° orientation the structure was expected to see higher loading because of the increased surface area, while simultaneously it had the shortest shear walls to carry the loads. The opposite was true for the 90° orientation where loading was decreased and shear wall capacity was increased.

Tables 1 and 2 show the average measured force from a variety of testing configurations. The overturning moment can be seen as positive values for the front load cells (LC2 and LC4 for 90°, LC2 and LC3 for 0°) and negative values for the rear load cells (LC1 and LC3 for 90°, LC1 and LC4 for 0°). This is found in all of the 0° trials as well as in the 90-1.0-WC-F-NE and 90-1.1-WC-

Table 1. Averaged Forces in Four Load Cells for Various Wave Lab Trials (0° Orientation)

Trial name	Wave height (cm)	Number of trials	LC1 (N)	LC2 (N)	LC3 (N)	LC4 (N)	LC Sum ^a (N)	Δ_{wave} (mm)
0-1.0-WO-F-NE	10	0	—	—	—	—	—	—
	20	4	−20	6	−39	−20	85	0.04
	30	0	—	—	—	—	—	—
	40	3	−85	81	177	−101	444	0.45
	50	0	—	—	—	—	—	—
	60	5	−167	322	457	−182	1,128	1.62
0-1.0-WC-F-NE	10	2	−34	6	2	−40	82	0.11
	20	2	−94	43	27	−103	267	0.68
	30	2	−123	137	69	−245	574	2.96
	40	4	−286	214	130	−343	973	3.90
	50	2	−403	413	254	−542	1,612	7.01
	60	3	−602	418	554	−617	2,191	4.69
0-1.1-WC-F-NE	10	2	−413	936	828	−263	2,440	3.75
	20	4	−240	436	346	−234	1,256	1.91
	30	2	−497	735	590	−309	1,231	4.62
	40	4	−755	936	1025	−552	3,268	9.51
	50	2	−958	1169	1070	−606	3,803	13.19
	60	2	−761	1296	1376	−1,012	4,445	13.43

^aAbsolute sum of LC1+LC2+LC3+LC4.

Table 2. Averaged Forces in Four Load Cells for Various Wave Lab Trials (90° Orientation)

Trial name	Wave height (cm)	Number of trials	LC1 (N)	LC2 (N)	LC3 (N)	LC4 (N)	LC Sum ^a (N)	Δ_{wave} (mm)
90-1.1-WC-NF-E	10	2	297	359	316	385	1,357	0.15
	20	7	643	808	695	845	2,991	0.10
	30	0	—	—	—	—	—	—
	40	9	814	1,064	847	1,162	3,887	0.53
	50	2	941	1,212	1,025	1,291	4,469	1.33
	60	10	1,034	1,329	1,104	1,410	4,877	1.79
90-1.1-WO-NF-E	10	0	—	—	—	—	—	—
	20	7	555	636	583	657	2,431	0.06
	30	2	671	988	752	886	3,297	0.09
	40	8	775	806	785	898	3,264	0.28
	50	2	680	839	716	919	3,154	0.24
	60	3	697	1,014	765	1,032	3,508	0.67
90-1.0-WNE	10	0	—	—	—	—	—	—
	20	0	—	—	—	—	—	—
	30	0	—	—	—	—	—	—
	40	8	-38	60	-72	31	201	0.10
	50	0	—	—	—	—	—	—
	60	7	-77	188	-121	100	486	0.30
90-1.0-WO-FN-NE	10	2	68	79	80	67	294	0.08
	20	4	164	197	182	206	749	0.07
	30	3	201	269	240	269	979	0.08
	40	4	261	329	326	331	1,247	0.13
	50	1	282	337	336	349	1,304	0.20
	60	4	199	342	233	368	1,142	0.27
90-1.1-WC-F-NE	10	2	-117	405	-142	258	922	0.20
	12	1	-105	411	-123	250	889	0.08
	15	1	-127	442	-107	263	939	0.10
	20	2	-55	287	-42	242	626	0.06
	30	2	-78	289	-46	181	594	0.14
	40	2	-78	364	-143	272	857	0.86
	50	2	-184	511	-232	292	1,219	1.13
	60	2	-182	539	-273	360	1,354	1.99

^aAbsolute sum of LC1+LC2+LC3+LC4.

F-NE trials as shown in Tables 1 and 2. Uplift was predominant only in three 90° configurations, as shown in Table 2, because all of the load cells have positive values indicating uplift. This was found to be the case whenever the base plate was not flashed.

Typically, force values were found to increase with increasing solitary wave height (H_{wave}), yet for two trials, this was not the case. In these trials, 0-1.1-WC-F-NE and 90-1.1-WC-F-NE, the force starts high, falls, and then continues to rise again with increasing wave height. This was due to smaller waves breaking near or on the structure. In Table 2, trial 90-1.1-WC-F-NE, it can be seen that two additional wave heights, 12 and 15 cm, were added. This was done in an attempt to see whether smaller waves break directly on the structure or not. It was observed that these waves do break near the structure. Deflection due to wave action (Δ_{wave}) in the 0-1.0-WC-F-NE and 0-1.1-WC-F-NE did not rise as much as expected between the 50- and 60-cm trials. This was because the LVDT used to measure deflections went over scale for these wave heights. Δ_{wave} for the 90° orientation is much smaller than that in the 0° orientation. This is due to combined effects of reduced loading in the 90° orientation (less surface area for loading) and stiffer shear walls (more than twice as long as the 0° orientation). The setup developed for the wave lab trials was

successful at capturing the force from wave loads on the 1/6th scale wood-framed structure. However, this setup was not suited for the direct measurement of lateral loads and overturning moments because exact location of the resultant of wave load could not be determined.

Behavior of Model Structure

The results that follow include a depiction describing the test conditions for those trials (Figs. 6–13) being discussed overlaid with the plots for that trial. The wave direction can be seen in each representation, accompanied by a directional compass. Some figures also have an x, y, z coordinate system to aid in the discussion that follows.

Elevated Structure: 90-1.1-WC-NF-E Configuration

The load cell data were averaged over all of the trials with the same wave height for this configuration and are shown in Fig. 6. Without an obstruction to water intrusion beneath the base plate there are predominantly uplift forces generated, with all four load cells in tension. The uplift and overturning behavior can be seen as the difference in magnitude between the front and rear load

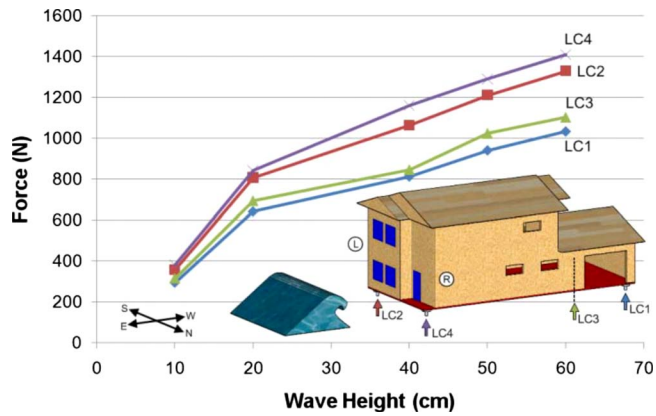


Fig. 6. Load cell data and depiction of test configuration for 90-1.1-WC-NF-E

cells. Furthermore, the differences between the two front load cells or two rear load cells can be seen to be differences in stiffness between the left and right side of the structure. Although push over tests (Wilson 2008) confirmed that the left side of the structure had greater stiffness than the right, LC4 has higher loading than LC2. This could be due to leveling errors when installing the structure or effects from the wave action on the reentrant

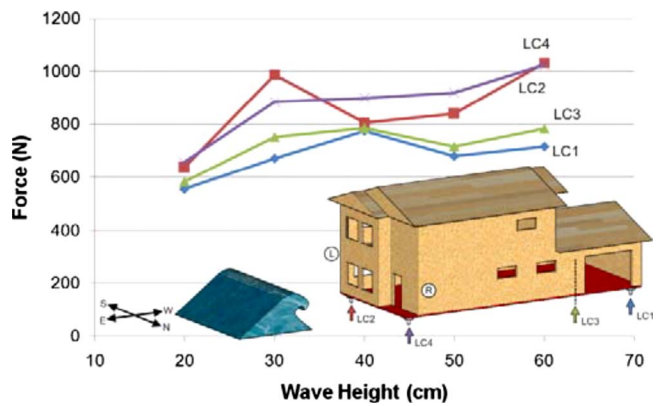


Fig. 7. Load cell data and depiction of test configuration for 90-1.1-WO-NF-E

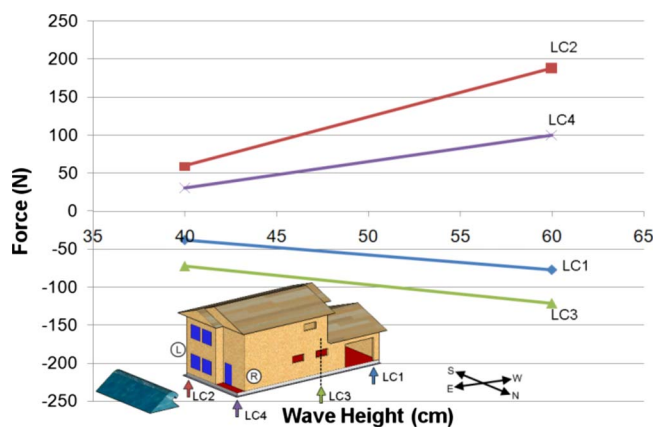


Fig. 8. Load cell data and depiction of test configuration for 90-1.0-WC-F-NE

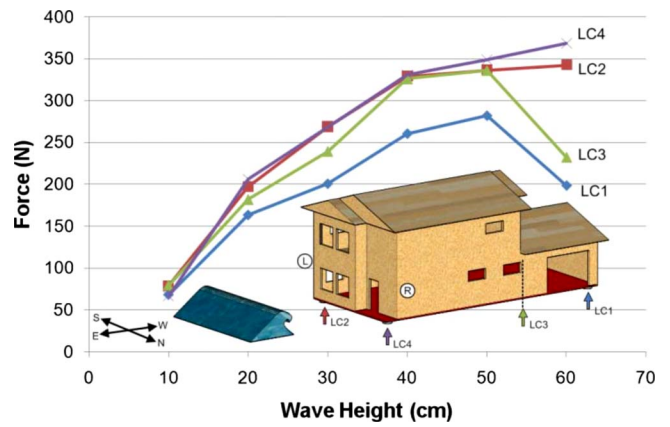


Fig. 9. Load cell data and depiction of test configuration for 90-1.0-WO-NF-NE

corner. For the 10-cm trial, the waves were not large enough to impact very high on the structure, with only uplift and smaller forces detected.

In a real world structure, similar force trends would be found indicating a need for special design considerations when examining this type of loading. Large uplift forces would necessitate stronger anchorage connections to keep the structure fixed to the foundation. It was seen in post-Katrina damage that several

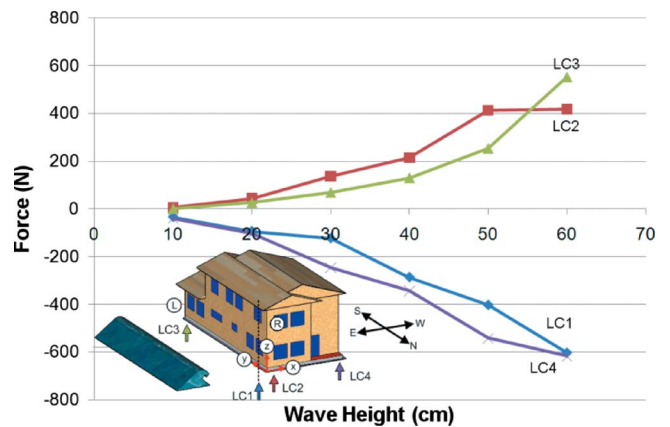


Fig. 10. Load cell data and depiction of test configuration for 0-1.0-WC-F-NE

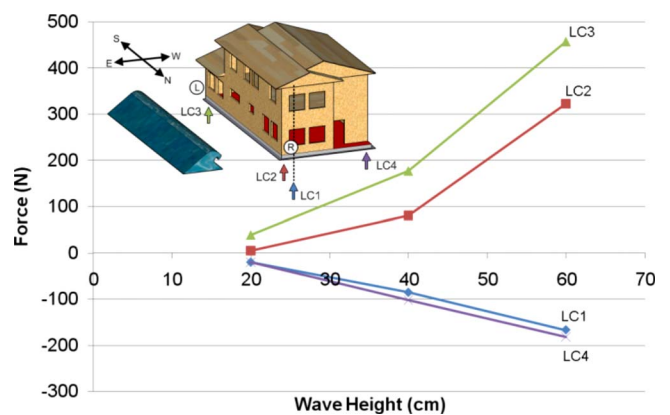


Fig. 11. Load cell data and depiction of test configuration for 0-1.0-WO-F-NE

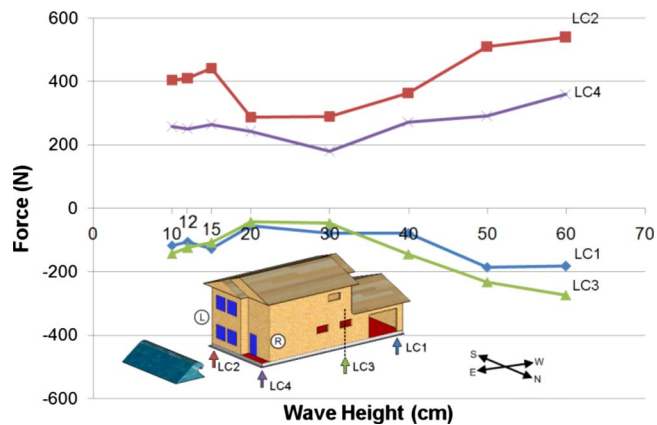


Fig. 12. Load cell data and depiction of test configuration for 90-1.1-WC-F-NE

homes were swept completely off their foundation from a combination of loading conditions, potentially including uplift of this nature. It should be noted that although the uplift forces are high, the horizontal impact loading on the structure would be reduced, as seen in Thusyanthan and Madabhushi (2008).

Elevated Structure: 90-1.1-WO-NF-E Configuration

Fig. 7 shows the averaged load cell data for this trial, where uplift forces are indicated by all load cells in tension, as well as the overturning behavior. The effect of removing the windows was to reduce the magnitude of the uplift forces, which could be seen as the combination of the effect of water applying a downward compressive force (once the water enters the structure through the windows) as well as less surface area on the front of the structure for loading. Window coverings in the model represent the situation where the home owner covered the windows with plywood, which is more likely with a hurricane where there is some advance warning of the storm. Absent window coverings could indicate a situation that required immediate evacuation more similar to a tsunami, where window glazing would be expected to fail under wave loading. This reduction in surface area might reduce the loading enough to allow the structure to survive as seen in Thusyanthan and Madabhushi (2008).

With open windows the real structure would see smaller uplift forces since water flowing through the structure would apply a

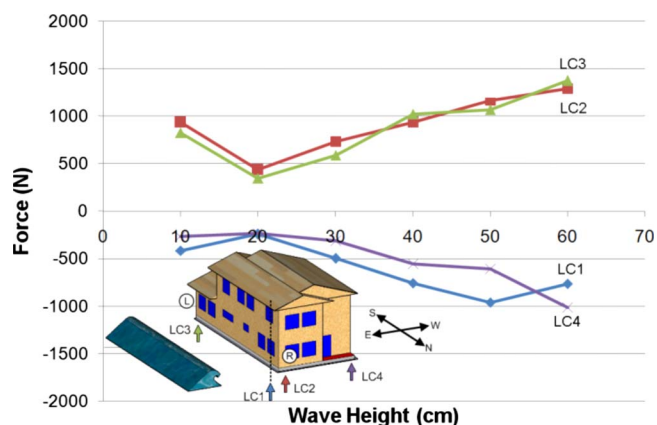


Fig. 13. Load cell data and depiction of test configuration for 0-1.1-WC-F-NE

downward pressure. This can be seen by comparing Figs. 5 and 6, where there is approximately a 25% reduction in force. This is not necessarily advantageous as the structure would face severe water damage, with interior nonstructural elements like drywall and carpeting destroyed. In the short term, if the reduction in forces allowed the structure to survive the initial impact it could protect immediate life safety and serve as shelter in the proceeding days. In addition, it is apparent that the force increases only slightly with increased wave height. It appears that larger waves send more water through the openings, which provides an increasing downward force with increasing wave height. Additionally, structures in coastal areas could be designed with interior elements in the lower stories to survive the water damage similar to areas with breakaway walls. It is clear that if a structure were designed to allow water intrusion beneath it the second story floor diaphragm should be as high as possible to prevent potential uplift and/or design proper anchorage.

Nonelevated Structure: 90-1.0-WC-F-NE Configuration

This configuration could be seen to model a slab on ground foundation or stem wall with no openings on the loaded face. Fig. 8 shows the averaged load cell data. The overturning moment is seen here as expected, with the front load cells in tension and the rear load cells in compression. Effects from the asymmetrical structural stiffness and reentrant corner can be seen as the difference in magnitude between the two front load cells and the two rear load cells. LC2 has a higher magnitude throughout the trials, which as discussed earlier was found to be due to the difference in stiffness from the left side to the right side of the structure. The left side is stiffer due to the longer second floor diaphragm on that side, combined with the large opening for the garage door on the right side, which reduces the stiffness on that side. Stiffness attracts load, thus it follows that the left side takes a higher portion of the loading. Data from the push over tests (Wilson 2008) indicated a similar trend.

This type of loading shows that the anchorage connections would be most vital on the side of the structure facing the oncoming waves. It is also clear that preventing water intrusion beneath the structure helps to reduce the uplift forces and thus the overall magnitude of the tensile forces are reduced. Typically when working with a flexible diaphragm (such as found in wood-framed buildings) it is assumed that the load is carried equally in each shear wall, this is not the case in this model. This is most likely due to a much stiffer floor diaphragm than would be seen in the full scale structure, yet clearly the shear walls do not equally carry loads between them.

Nonelevated Structure: 90-1.0-WO-NF-NE Configuration

This structural configuration simulates an open “crawl space” (under floor space), as depicted in the lower right corner of Fig. 9. The averaged load cell data for this trial can also be seen in Fig. 9, which shows predominantly uplift forces. The overturning behavior is not obvious in this trial. For the 10- and 20-cm wave heights, the bore height (crest to trough height of broken wave) reached just above the steel plate, generating only uplift due to the water running under the plate. For larger wave heights some difference in magnitude is seen between the front and rear load cells, but not until the 60-cm wave does this difference clearly indicate the overturning moment expected. Smaller waves hit the full width of the structure for loading because they are hitting below any window openings, but as the waves get higher, the window openings reduce the surface area available for the waves. However, the 60-cm wave was seen to hit the structure above first

story window and door openings, thus having the full width of the structure for loading in that region. This is thought to be why LC1 and LC3 decrease, showing the overturning moment more clearly with the largest wave.

This wave trial is difficult to analyze due to the many changing variables. As water moves beneath the plate uplift of the plate occurs, yet with openings in the structure, water can also travel across the top of the plate potentially reducing this force. Furthermore, the window openings give different surface areas for loading depending on the height of the bore. Clearly, uplift is the dominant portion of the loading. Windows open with a flashed base plate were not tested, which would have allowed further isolation of these variables from the uplift forces for analysis. As was stated in earlier discussion, if water is allowed beneath the structure the horizontal wave loading would be reduced, as was found in Thusyanthan and Madabhushi (2008). Additionally, the openings in the structure would further reduce this loading, as there is less surface area for loading. Again special design of anchorage would need to be considered.

Nonelevated Structure: 0-1.0-WC-F-NE Configuration

The structure tested is depicted in the lower left corner of Fig. 10. Here the overturning moment is prominent, and as expected rising force follows rising wave height. One exception is with LC2 during the 60-cm wave trials, which has no increase in loading between the 50- and 60-cm trials. The smallest wave, 10 cm, was only high enough to strike the flashing beneath the steel plate and thus provided little loading for the actual structure.

As indicated by push over tests (Wilson 2008) the right side has greater stiffness than the left side, and therefore attracts a higher portion of the loading. It would then be expected that LC2 and LC4 would have a higher magnitude of loading than LC1 and LC3. Yet in the largest wave LC2 drops in magnitude. This was found to be due to the first story overhang above the garage. The largest waves were applying an upward vertical force to this eave, evident not only from observation, but also in the loosening of the plywood roofing on this side. This would indicate strong uplift forces applied on the front left corner above LC3. This upward force at the left side of the structure would cause an additional overturning moment, rotating the structure in the y - z plane as indicated by the coordinate axis in Fig. 10. This additional moment would cause the front right load cell (LC2) to decrease in magnitude and the front left (LC3) to increase in magnitude, which is what the data indicate.

Nonelevated Structure: 0-1.0-WO-F-NE Configuration

Fig. 11 shows the averaged load cell data, where the overturning moment is indicated as expected. There are fewer wave heights for this trial, e.g., only 20, 40, and 60 cm, yet each wave height had three or more replicates compared to many other configurations which had only two replicates.

Given that the right side of the structure is stiffer than the left, it is not clear why LC3 would have a greater magnitude of force than LC2. The previous trial clearly indicated the opposite trend and the only variable changed was the opening of the windows, so the answer must lie with water intrusion through the openings. There are two additional windows on the front right corner (on the narrow face of the structure) where water was seen to enter during testing. It is likely that more water enters at the right side lowering the tensile forces on that side. Further testing would be necessary to fully isolate the effects of changing window coverings but it is clear from test data that the magnitude of the forces are decreased disproportionately to the reduction in surface area.

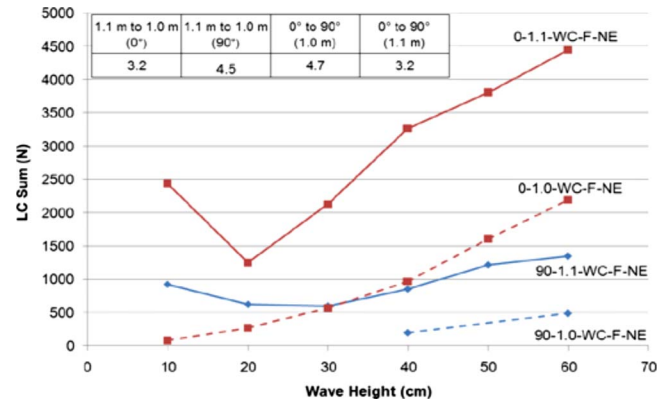


Fig. 14. Force plotted as LC Sum comparing wave height and orientation

Submerged Structure: 90-1.1-WC-F-NE Configuration

This configuration had the same setup as that depicted in Fig. 8, except the water level was raised to 1.1 m leaving the structure partially submerged. The collected load cell data shown in Fig. 12 indicate an increase in loading for the waves around 10–15 cm in height. This was followed by a decrease in loading when the wave height was increased.

It was found that the smaller waves were breaking on or very near the structure. To this end, 12- and 15-cm trials were added to investigate waves breaking directly on the structure. Since waves lose energy when they break, a breaking wave on the structure would impart higher loading. As the wave heights increased the waves broke further off shore and this explains the reduced loading. Once the waves had broken offshore the force increases with increasing wave height as expected. Trends found in the 90-1.0-WC-F-NE trial are repeated here with higher loading values due to the increased water depth. Again the overturning moment is generated, and again the front right load cell (LC4) sees a decrease in loading, which would be an indicator of higher structural stiffness on the left side.

Submerged Structure: 0-1.1-WC-F-NE Configuration

This configuration (Fig. 13) is identical to that found in Fig. 10, with an increase in water depth to 1.1 m. Correspondingly, there are higher forces in these trials, seen by comparing Fig. 10 with Fig. 13. The load cell values, shown in Fig. 13, were higher for 10-cm waves than for the next two waves (20 and 30 cm) and almost same as the 40-cm waves. The higher loading by the 10-cm wave compared with 20- and 30-cm waves was caused by the fact that the 10-cm waves break at or near the structure.

This is the structural configuration that ultimately failed the structure. Loading was highest in these trials since the water depth was increased and the structure was oriented with its largest face to the oncoming waves and windows closed. Trends found in the 0-1.0-WC-F-NE trial are repeated here, with higher loading values due to the increased water depth. The overturning moment is clearly indicated, as well as differences in magnitude between load cells due to stiffness irregularities. The 60-cm trial again shows a decrease in loading on the right side, indicative of the loading applied to the eaves on the left side of the structure.

0° versus 90°

In comparing the 0° and 90° orientation, the most regular structural configuration is examined, i.e., windows closed, flashed base plate, and a nonelevated condition. Fig. 14 shows a comparison

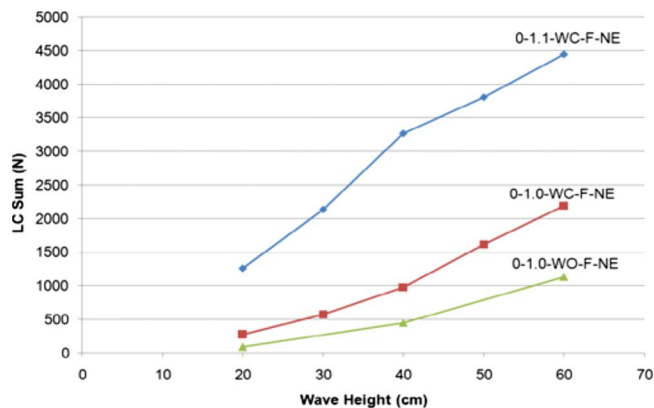


Fig. 15. Force plotted between the 0-1.1-WC-F-NE, 0-1.0-WC-F-NE, 0-1.0-WO-F-NE configurations

between the 0° orientation and the 90° orientation, in both 1- and 1.1-m water depths. For these plots, the four load cell values were summed as absolute values, as an indication of the total force at a given time. As expected, the 0° orientation has larger total force when compared to the 90° orientation. However, when total load is normalized by the width of the structure it is still higher for the 0° orientation compared to the 90° orientation. The aspect ratio of the structure is approximately 2:1, yet the difference in load is approximately 3:1 from the 0° to the 90° orientation in both water levels. There are a variety of forces during wave loading, including buoyant, surge, drag, and hydrostatic forces. It is probable that other loading effects are causing the discrepancy in loading between the 0° and 90° orientations.

Open Windows versus Closed Windows

To examine the effects of open windows versus closed windows more closely, load cell sum was plotted against the wave height (H_{wave}) for the 0-1.0-WC-F-NE and 0-1.0-WO-F-NE trials, as seen in Fig. 15. With windows opened, water travels through the structure adding a compressive force as well as reducing the available surface area for loading. The ratio of force from the windows closed condition to the windows open condition is about 2.5:1. Although the surface area for loading is different depending on the runup for a given wave, the windows account for $\sim 25\%$ of the first story surface area in the 0° orientation. This reduction in loading is significant, and could mean the survival of a structure as seen in the paper by Thusyanthan and Madabhushi (2008).

Flooded versus Nonflooded

Testing took place with a water level of 1.0 m and 1.1 m. To compare these two conditions, the combined load cell data are examined over varying wave heights for the 0-1.1-WC-F-NE and 0-1.0-WC-F-NE trials, as seen in Fig. 15. The wave data below 20 cm are eliminated in this case to avoid the breaking wave condition present only during the 1.1 m water level. The addition of 10 cm of water provides a significant addition of force and represents a flooded condition similar to that seen during hurricanes. The ratio of force from the flooded to the nonflooded trials was approximately 3:1 in the 0° orientation. It is interesting that as H_W increases the difference between the forces also increases, as seen in Figs. 13 and 14.

Conclusions

This study was successful in both meeting its objectives as well as laying the groundwork for the methodology and guidelines of future studies. As there is very little research in this area, one of the major accomplishments was to successfully setup a scale experiment to capture force and deflection of a realistic compliant model.

This paper presented the structural response to many different testing conditions. This qualitative approach showed that (1) differences in structural stiffness throughout the structure will cause a different load distribution on the output reactions, (2) architectural features, e.g., overhanging eaves above the garage and reentrant corners, can provide unanticipated loading conditions, (3) if water travels beneath the structure, uplift becomes the predominant component of loading, and (4) the effect of waves breaking on or near the structure greatly increases the loading.

By comparing configuration changes in the different trials, it was found that the difference in loading from the 0° to 90° orientation averages approximately 3:1. Since the aspect ratio of the structure is approximately 2:1, this is at odds with wave loading equations, which assume a uniform force per unit width, and will thus require further investigation. The ratio of force from the windows closed condition to the windows open condition is approximately 2.5:1. The ratio of force from the 1.1 m water depth to the 1.0 m water depth averages approximately 3.8:1. There are a variety of forces during wave loading, including buoyancy, surge, drag, and hydrostatic forces, which are likely causing the discrepancy in loading between the different trial orientations.

In the flooded condition, the forces were much higher than in the nonflooded condition. In addition, residential coastal structures vary in architectural design, thus it is important to develop methods for determining wave loads taking into consideration the shape of the structure. It was found that opening the windows and doors reduced loading by 60%. This indicates a need to further investigate special designs for coastal structures to reduce wave loading, similar to work done by Thusyanthan and Madabhushi (2008). Wave loading is complex and large differences can be seen with small changes in structural configuration and coastal conditions, clearly necessitating the need for further research to develop accurate and reliable engineering design guidelines.

Acknowledgments

This research was supported, in part, by a grant from the National Science Foundation under Grant Nos. CMMI-0530759 (NEES Research) and CMMI-0402490 (NEES Operations). This support is gratefully acknowledged. Any opinions, findings, and conclusions or recommendations expressed in this material are those of the investigators and do not necessarily reflect the views of the National Science Foundation. The authors are also grateful to the PBTE NEESR Hireef Project Group (from Hawaii) and the NEES@OSU site personnel for their cooperation and assistance, respectively. The research was also supported, in part, by the Forest Research Laboratory General Funds and Center for Wood Utilization Special Research Grant funds available through the Department of Wood Science and Engineering at Oregon State University. In addition, prefabrication of the structural models was performed by Mr. Doug Allen, an undergraduate research assistant at Colorado State University. His skill and participation on the project is acknowledged. The writers also thank Dr. Dan Cox, Director, O. H. Hinsdale Wave Research Laboratory, for

providing help during the experimental phase of the project and in preparation of this manuscript.

References

- American Forest and Paper Association (AFPA). (2006). *Guide to Wood Construction in High Wind Areas for One- and Two-Family Dwellings—130 mph Exposure B Wind Zone*, Washington, D.C.
- Arnason, H. (2005). “Interactions between an incident bore and a free-standing coastal structure.” Ph.D. thesis, Univ. of Washington, Seattle.
- ASCE. (2005). “Minimum design loads for buildings and other structures.” *ASCE/SEI 7-05*, Reston, Va.
- FEMA. (2005). “Coastal construction manual: Principles and practices of planning, siting, designing, constructing, and maintaining buildings in coastal areas.” *FEMA 55*, 3rd Ed., Washington, D.C.
- Garcia, R. (2008). “Wave and surge loading on light-frame wood structures.” MS thesis, Colorado State Univ., Fort Collins, Colo.
- Goring, N. D. (1979). “Tsunamis—The propagation of long waves onto a shelf.” *Rep. No. KH-R-38*, W. M. Keck Laboratory, California Institute of Technology, Pasadena, Calif.
- HBC. (2000). *Department of Planning and Permitting of Honolulu Hawaii. City and County of Honolulu Building Code, Chapter 16, Article 11*, Honolulu, (<http://www.co.honolulu.hi.us/Refs/ROH/16a1.htm>).
- National Weather Service. (2005). “Hurricane Katrina, a climatological perspective.” *Technical Rep. No. 2005-01*, National Oceanic and Atmospheric Administration, National Weather Service, Silver Spring, Md.
- Ramsden, J. D. (1993). “Tsunamis: Forces on a vertical wall caused by long waves, bores, and surges on a dry bed.” *Rep. No. KH-R-54*, W. M. Keck Laboratory, California Institute of Technology, Pasadena, Calif.
- Su, C. H., and Mirie, R. M. (1980). “On head-on collisions between two solitary waves.” *J. Fluid Mech.*, 98(3), 509–525.
- Thusyanthan, N. I., and Madabhushi, S. P. G. (2008). “Tsunami wave loading on coastal houses: A model approach.” *New Civ. Eng. Int.*, 161(2), 77–86.
- van de Lindt, J. W., Graettinger, A., Gupta, R., Skaggs, T., Pryor, S., and Fridley, K. J. (2007). “Performance of wood-frame structures during Hurricane Katrina.” *J. Perform. Constr. Facil.*, 21(2), 108–116.
- Wilson, J. (2008). “Behavior of a 1/6th scale, two-story, wood-framed residential structure under surge wave loading.” MS thesis, Oregon State Univ., Corvallis, Ore.
- Wydajewski, K. J. (1998). “Response of breakaway walls to hydrodynamic wave loading.” MS thesis, Oregon State Univ., Corvallis, Ore.
- Yeh, H., Robertson, I., and Preuss, J. (2005). *Development of design guidelines for structures that serve as tsunami vertical evacuation sites*, National Tsunami Hazard Mitigation Program, NTHMP, Seattle.